

Measurement Evaluation and Simulation of an Innovative Drainback Solar Combi-System

Yoann Louvet¹, Janybek Orozaliev¹ and Klaus Vajen¹

¹ University of Kassel, Institute of Thermal Engineering, Kassel (Germany)

Abstract

This paper presents an innovative drainback solar combi-system constructed in a new building during the year 2016. The system is unpressurized, and the same heat transfer fluid circulates from the solar collectors to the air-handling unit delivering the heat to the building. The number of heat exchangers is thereby minimized. The first measurement data show a lower system performance than expected, which can be explained on the one hand by differing heat demand compared to what was originally planned and on the other hand by improvement potentials, especially regarding the control strategies. TRNSYS simulations highlight that simple modifications of the control strategy could more than double the saved final energy. Detailed calculations nevertheless show that heat costs ($LCoH_{ov,fin}$) still remain between 24.5 and 30 % higher compared to a conventional heating system.

Keywords: combi-system, drainback system, passive house

Nomenclature

ΔQ_{st} : variation of the store internal energy in kWh
 A, B, C and D: fit parameters of the sigmoid function $h(T_{amb})$
 A_a : collector aperture area in m^2
 A_G : collector gross area in m^2
 $f_{sav,ext}$: extended fractional energy
 $f_{sav,ext}$: extended fractional energy savings
 $f_{sav,th}$: fractional thermal energy savings
 I_0 : investment costs in €
 $LCoH_{ov,fin}$: levelized cost of heat of the entire system based on final energy in €/kWh
 Q_{bal} : store energy balance in kWh
 Q_{boil} : energy delivered by the boiler to the store in kWh

Q_{DHW} : energy delivered to the domestic hot water loop in kWh
 $Q_{loss,p}$: heat losses of the piping in kWh
 $Q_{loss,st}$: heat losses of the store in kWh
 Q_{SH} : energy delivered to the space heating loop in kWh
 Q_{sol} : energy delivered by the solar collector loop to the store in kWh
 $T_{amb,d-1}$: mean ambient temperature of day d-1 in °C
 T_{amb} : mean ambient temperature in °C
 $T_{boil,set}$: boiler set-point temperature in °C
 $T_{SH,set}$: space heating set-point temperature in °C
 $T_{st,1..5}$: store temperature in °C (1 = bottom, 5 = top)

1. Introduction

The reduction of the costs of solar thermal systems is a key issue to limit the reduction of the market which is currently faced in Europe. One approach to achieve this target is to simplify the design of solar thermal systems to reduce the number of components, therefore reducing investment costs and the resulting maintenance. The drainback design without heat exchanger in the collector loop is for this purpose an appropriate solution. An extensive analysis of the advantages and drawbacks of drainback systems (DBS) can be found in Botpaev et al. (2016). The combi-system presented in this study is an attempt to push the drainback concept at its limit, by placing the heat storage in the attic directly below the collectors. This allows getting rid of most of the issues linked to the drainback design. It furthermore allows an unpressurized boiler operation, further reducing the number of heat exchangers in the system.

In a first step the hydraulic configuration and the control strategy of the studied system are described in the details. A reference conventional system, without solar assistance is also defined. The evaluation of the monitoring campaign carried over one and a half year is then presented. The energy balance as well as the load profiles are analysed. Several issues hampering a proper functioning are identified and solutions proposed.

Based on these measurement, a simulation model was developed in TRNSYS (Klein et al., 2006). The impact of several control and design improvement measures on the system performance is assessed. The impact of varying load profiles is also evaluated. In a last step, the heat costs ($LCoH_{ov,fin}$) are calculated and compared to the ones of the reference conventional heating system.

2. Description of the studied system

The studied solar combi-system consists of a 13.8 m² (aperture area) evacuated tubular collector field with heat pipes (VITOSOL 200-T from Viessmann) and a 1 m³ polypropylene (PP) heat storage (from Enersolve GmbH). The collectors, presenting a total aperture area (A_a) of 13.84 m², are directly installed on the roof with a slope of 20° and an azimuth of S53°W. It is equipped with a 35 kW gas condensing boiler (VITODENS 300-W from Viessmann) as back-up heater and provides space heating (SH) and domestic hot water (DHW) to a new multi-functional building, used as boathouse, changing room as well as seminar room by the University of Kassel. The building has a total floor area of 268 m² and is built as passive building. During the planning phase, a primary energy need of 8.6 MWh/a for space heating and 6.9 MWh/a for DHW were foreseen.

The hydraulic scheme of the system is depicted in Fig. 1. Its innovative character lies in the fact that it is an open, i.e. non-pressurised system with very few heat exchangers, thereby saving costs and increasing the system efficiency. The same heat transfer fluid (HTF), water with a corrosion inhibitor, circulates from the solar collectors to the air-handling unit delivering most of the heat to the building. Some additional radiators are installed, also supplied by the same HTF. DHW is provided by a fresh-water unit. The solar collector loop is designed according to the drainback principle in order to avoid freezing of the water in winter. The heat storage, the boiler, the fresh-water unit and the air-handling unit (AHU) are all located directly below the roof in the attic. This is an advantage for the DBS as the apex of the solar collector loop is located approximately 1 m higher than the water level in the store. This avoids the need for pump oversizing for filling at start-up and also minimizes underpressure in the collectors during operation. The air volume of the heat storage is directly connected to the atmosphere. It was necessary to adapt the internal control strategy of the boiler in order to allow non-pressurised operation.

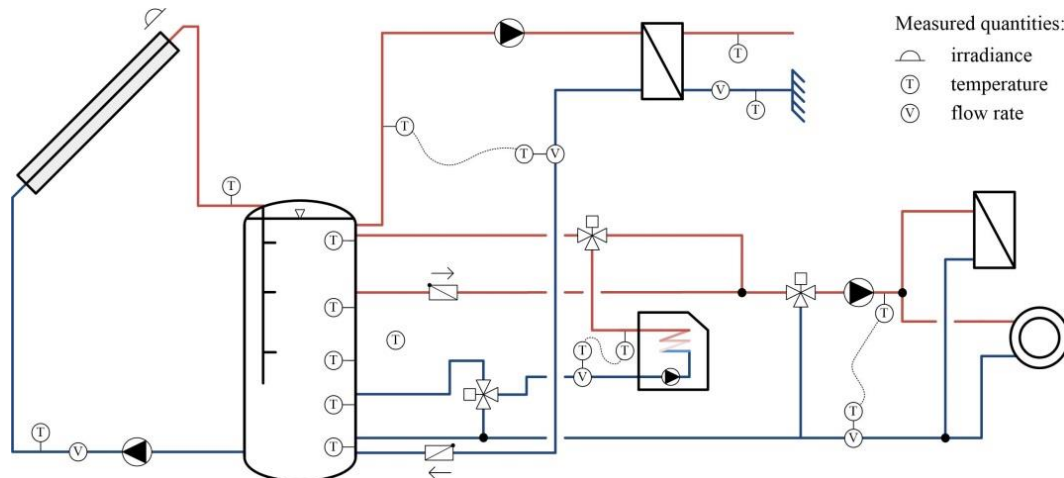


Fig. 1: Schematic hydraulic drawing of the unpressurised combi-system studied with the installed measurement instrumentation.

Concerning the control strategy, several improvements were achieved during the monitoring period. From the initial parametrisation several points have to be noticed. The solar collector loop pump starts when the temperature difference between the bottom of the tank and the collector exceeds 12 K and stops when it falls below 3 K. To avoid too high stresses which could reduce its lifetime the store temperature is limited ($T_{st,1}$ limited to 70 °C and $T_{st,4}$ limited to 85 °C). Regarding the load, a DHW volume of 370 litres (until the 4th temperature sensor in the store, $T_{st,4}$) is kept at a set temperature of 60 °C (± 2 K), and the motor valve situated in the return pipe of the boiler allows the preparation of a larger DHW volume on-demand; a button to be pushed manually is located in the changing rooms for this purpose. Finally the set-point temperature for space heating depends on the ambient air temperature. It is determined by the controller of the AHU and communicated to the boiler. On weekdays between 7:00 and 22:00 the set-point temperature has a fixed value of 57.5 °C during the heating season.

10	Measurement devices	Presence of air bubbles in the flow metre of the HFM.	Move flow meter from the flow side to the return side of the boiler.
11	Measurement devices	Accuracy and reliability of the Grundfos Vortex VFS sensors.	Prefer other types of sensor.
12	Measurement devices	Incoherent storage temperatures.	Use longer immersion sleeves.
13	Maintenance	One valve forgotten in close position, preventing DHW use.	Careful check of the manipulated hydraulic components after maintenance.

3.2. Energy balances

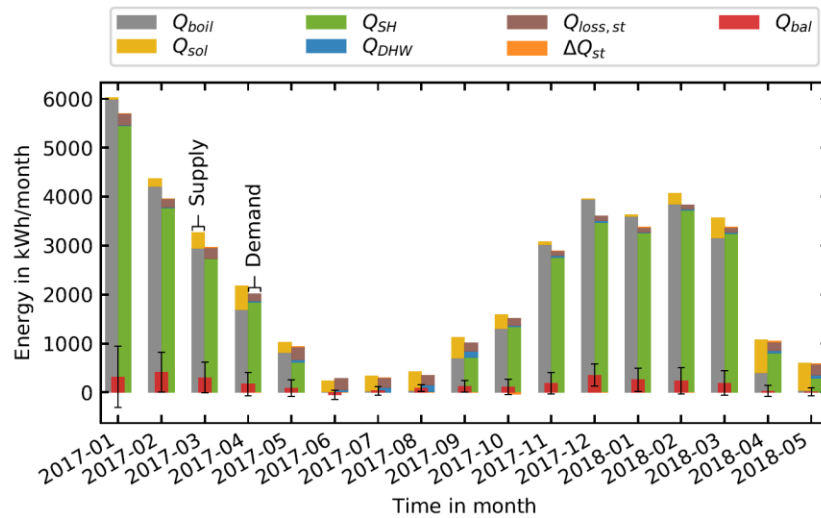


Fig. 3: Monthly energy supply and demand at the boathouse for heating as well as monthly balance including measurement uncertainties (95 % confidence). Data between January 2017 and May 2018.

The heating energy input and output of the system are presented on a monthly basis over the monitoring period in Fig. 3. Because of the issues above-mentioned, the following points have to be clarified:

- Due to the problem with the heat metre in the boiler loop, the energy delivered by the boiler could not be directly measured until the beginning of June 2017. The energy delivered by the boiler before this date is estimated from the measured gas consumption. A boiler utilization ratio of $90.2 \% \pm 5.5 \%$ -point (95 % confidence) is calculated for the heating season. This value is used to calculate the monthly Q_{boil} between January and May 2017.
- Until the 11th of July 2017 the DHW demand was only measured on the secondary side of the heat exchanger of the fresh water unit. Due to the heat exchanger losses but mainly to the thermosiphonic circulation observed and described before, the actual heat delivered by the storage to the DHW loop is expected to be significantly higher than the energy measured on the secondary side of the heat exchanger. Due to the lack of better data, the energy delivered to the DHW loop until this date was set equal to the energy measured on the secondary side of the heat exchanger. Over this period, the heat loss coefficient of the heat storage was however corrected to include the losses due to the thermosiphonic circulation, as explained in the next point.
- The heat loss coefficient of the heat storage is estimated based on measured data. During the period when thermosiphonic circulation occurred, before the check-valve was installed, two heat loss coefficients were calculated, one including the losses from the thermosiphonic circulation and one excluding them, respectively $9.3 \text{ W/K} \pm 2.0 \text{ W/K}$ and $6.9 \text{ W/K} \pm 1.1 \text{ W/K}$ (95 % confidence).

The monthly values show a typical profile for a combi-system, where most of the demand occurs during the winter months for space heating. During the summer months, the supply is almost exclusively covered by the

solar thermal system. Over the studied period, the DHW needs represented 2.0 % of the total energy demand, while the SH needs accounted for more than 90 % of the total. On the supply side, most of the energy was delivered by the gas boiler (88 %). Compared to the energy demand foreseen during the design phase of the building, one can notice that for the year 2017 the DHW needs are far below the expected values (10.4 times lower), and on the contrary the space heating demand is 2.9 times higher than originally planned. A primary energy factor of 1.1 is assumed to compare the foreseen primary energy needs with the measured consumptions (Deutscher Bundestag, 2016). The unexpected demands are discussed more in details in the following sections.

3.3. Space heating demand

The daily space heating demand of the building is shown in Fig. 4 as a function of the average ambient temperature. The sigmoid function used to approximate the scatterplots is described in Hellwig (2003) and is presented in eq. (1). The average ambient temperature considered is a geometric construction, as recommended by BDEW (2015) and expressed in eq. (2).

$$h(T_{amb}) = \frac{A}{1 + \left(\frac{B}{T_{amb} - 40}\right)^C} + D \quad (\text{eq. 1})$$

$$T_{amb} = \frac{T_{amb,d} + 0.5 \cdot T_{amb,d-1} + 0.25 \cdot T_{amb,d-2} + 0.125 \cdot T_{amb,d-3}}{1 + 0.5 + 0.25 + 0.125} \quad (\text{eq. 2})$$

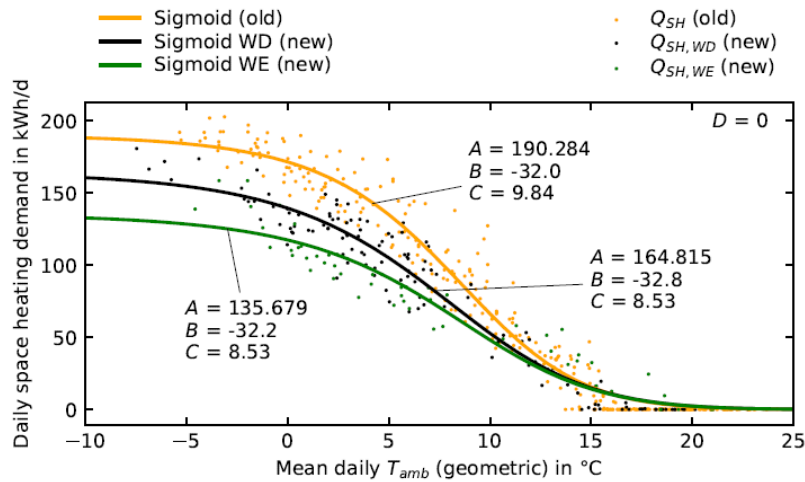


Fig. 4: Measured daily space heating demand between November 2016 and Mai 2018 and sigmoid functions approximating the demand with their coefficients.

In the interpolated curves D is set to zero as only the space heating demand is considered for the boathouse, while eq. (1) represents the total heat demand including the DHW needs. The measured data shows a clear difference of the SH demand before (old) and after (new) correction of the issues which caused high inlet temperatures to the SH loop; No. 6 and 7 notably (Tab. 1). The daily SH needs are impacted by the corrections in two ways: (a) the daily needs are generally lower than before the correction (orange data), and (b) weekdays (black data) and weekend days (green data) present differentiated profiles. Point (a) can be explained by the fact that the inlet temperature to the SH loop was always higher than required. After correction, the boiler reaches its lower power threshold much more often (especially at night and during the weekends when the set-point temperature is low) which causes repeated on/off boiler cycling. For this reason, the AHU receives a fluctuating inlet temperature, which drops cyclically for a few minutes (with a typical frequency of 15 minutes) a few degrees below the set temperature. As a consequence, the measurements show that during nights and weekends, the rooms do not keep a temperature of 21 °C as it was the case before the correction, and their temperature drop depending on the outside temperature (room temperatures close to 18 °C were measured as a minimum during winter 2017-2018). Point (b) is a consequence of (a) and the differentiated set-point temperatures during weekends and weekdays. An insufficient number of measurement points were available to properly estimate the new heating curve on the weekends. For this reason, it was decided to constrain some of the parameters of eq.(1) for its calculation. As mentioned in Hellwig (2003), the sigmoid plateaus for the extreme cold temperatures due to the dimensioning of the heating system, which corresponds to A. In the case of the boathouse, the orange and black heating curves highlight that this threshold is also impacted by the control

strategy of the heating system as illustrated hereinabove. It is hence not realistic to fix A. However the flattening of the old and new weekday sigmoid curves expressed by the coefficient C is similar. For the new heating curve on weekend days C is hence set equal to the new heating curve on weekdays. Finally due to the shape of the sigmoid curve, a residual daily space heating demand is always present even at high mean ambient temperature. This is not realistic, especially during the summer months and it can be clearly seen on the graph that there is often no SH demand when the ambient temperature exceeds 15 °C. To avoid this effect, the daily space heating demand is set to zero outside of the heating season (from May 15 to Sep. 15) when the geometric mean ambient temperature is higher than 15 °C. The daily SH demand calculated with the new sigmoid curves is then compared to the measured consumption in Fig. 5. Both curves follow a similar trajectory, nevertheless the model shows less rapid oscillations than the measured curve. For this reason, peaks of demand often have lower amplitude in the model compared to the reality.

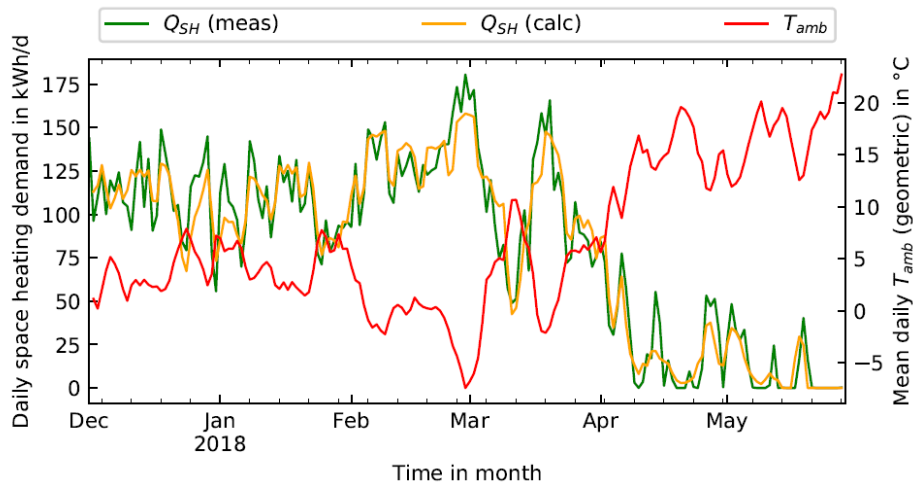


Fig. 5: Comparison of the measured and calculated daily SH demand and geometric mean daily temperature.

During the year 2017, the space heating demand was almost 3 times higher as foreseen during the planning phase despite 2 % less degree days compared to the long-term average¹. A detailed analysis of additional data from the AHU shows high air exchange rates with the outside through the AHU during the heating season, even at night or when the building is not occupied, which explains despite the air heat recovery unit the high losses to the ambient.

3.4. Domestic hot water demand

The DHW demand was surprisingly low over the studied period compared to what was foreseen during the planning of the building. After questioning supervisors of the people utilizing the building (for sports training), came out several reason for this low DHW demand:

- most people come to the boathouse with bikes, therefore prefer not to shower there but rather at home
- the two locker rooms are too small and only 5 to 6 people can change per room at the same time (while four showers per room are available)
- so far only few activities take place at the boathouse, more are planned in the future.

On top of that, during the first months of 2017 hot water was not available during several weeks. The confidence of the users in the possibility to shower was for this reason reduced. However the supervisors mentioned that users should currently be aware that the system is functioning.

The low DHW demand is responsible for the poor performance of the solar thermal system during the summer months. Between June and August 2017 (3 months) collector stagnation occurred 53 days. Overall in 2017 the

¹ Degree days calculated with the Excel tool provided by IWU (2018) for the weather station Fritzlar, data for Kassel not been available. The method Gradtagzahl is selected for an internal temperature of 20 °C and a heating threshold-temperature of 12 °C. The long-term average refers to the period 2002-2017.

solar energy yield delivered to the heat storage amounts to $212.6 \pm 17.4 \text{ kWh/m}^2(A_a)/a$, which is a quite low value for a combi-system.

Because of the low demand, it appeared unnecessary to maintain a 370 litres DHW volume at $60 \text{ }^\circ\text{C}$ all the time. The DHW volume was thus reduced to 110 litres, corresponding to the position of the 5th temperature sensor in the tank. It should be noticed that no DHW volume was foreseen in the original planning. Instead the users should have manually activated DHW preparation before their sport activities so that they could shower one or two hours later. The building operator finally decided not to retain this solution and to always maintain a DHW volume in the store.

4. System simulations and improvement potential

The following simulations are carried out with TRNSYS 16.01 (Klein et al., 2006). The measured load profiles are replaced with synthetic load profiles to allow variations. The SH profile is generated on an hourly basis with the data presented in the previous section. For DHW, the software DHWCalc allowing the generation of random load profiles is applied with a daily consumption of 40 l at $45 \text{ }^\circ\text{C}$ approximately corresponding to the measured yearly DHW consumption (Jordan and Vajen, 2005). These profiles result in a total simulated yearly consumption of 19.68 MWh/a for SH and 0.58 MWh/a for DHW. Concerning the weather file the measured data from the year 2017 are used as model input. The yearly solar irradiation in the collector plane amounts to $1022 \text{ kWh/m}^2/a$ and the yearly mean ambient temperature to $10.7 \text{ }^\circ\text{C}$. The results of the simulations were compared with the measured values over the first four months of 2018 and showed a good agreement.

4.1. Impact of various parameters on the system performance

A reference solar thermal heating system is first of all defined. All issues related to the design and control of the system (except No. 8) as they are presented in Tab. 1 are considered as part of the reference. The parameters listed in Tab. 2 are then varied one after the other to assess their potential for system performance improvement. Parameters related to the control strategy range from *a* to *f*, while the ones from *g* to *j* are linked to the system design. Concerning the control strategies, store prioritisation (*a*) is achieved by decreasing the boiler set-temperature to a low value (below $10 \text{ }^\circ\text{C}$) when $T_{st,4} > T_{SH,set}$, which prevents it from running. A reduction of the size of the DHW volume (*e* and *f*) is furthermore tested as it better suits the low demand. The simulation without DHW volume (*f*) reproduces the behaviour foreseen in the real system. The boiler heats up the heat storage during 30 minutes before a drawing, as long as $T_{st,2}$ does not exceed the set-point. With regards to the design of the system, higher collector tilt angles (*i*) are simulated as 20° seems relatively low for a combi-system. The impact of improved storage insulation is also assessed (*j*). Finally the impact of the simultaneous variation of several parameters is also evaluated.

Tab. 2: List of the modifications implemented in TRNSYS to assess their impact on the system performance.

No.	Parameter modified	Addressed issue
<i>a</i>	Boiler stops delivering to the DHW loop when $T_{st,4} > T_{SH,set}$	5
<i>b</i>	$T_{boil,set}$ reduced when low SH demand during the day	6
<i>c</i>	Boiler outlet temperature corrected from offset	7
<i>d</i>	$T_{st,1,max}$ increased from $70 \text{ }^\circ\text{C}$ to $80 \text{ }^\circ\text{C}$	9
<i>e</i>	Size of the DHW volume reduced till the height of the 5 th (top) temperature sensor	
<i>f</i>	No DHW volume, only one button for DHW on demand	
<i>g</i>	Ideal store stratification	1
<i>h</i>	Smaller boiler (19 kW, minimum power of 1.7 kW)	2
<i>i</i>	Collector tilt increased (<i>i1</i> : 25° , <i>i2</i> : 30° , <i>i3</i> : 35°)	
<i>j</i>	Store insulation improved (<i>j1</i> : class D, <i>j2</i> : class C, <i>j3</i> : class B)	

The outcome of the simulations is summarized in Fig. 6. The two fractional energy savings are presented, as well as the yearly collector yield (directly between the collector field inlet and outlet), the store losses and the pipe losses in the solar collector loop. Energies are given as specific values, relative to the collector aperture area. The results are presented by issue type (control / design) and ranked by rising $f_{sav,ext}$.

The reference conventional heating system against which all solar thermal systems are compared present store losses of $51 \text{ kWh/m}^2(A_s)/a$ and the total heat delivered by the boiler amounts to 21.82 MWh/a . It is first of all to notice that as one could expect, the multiple issues above mentioned significantly hamper the performance of the reference solar thermal system. It reaches an extended f_{sav} of 7.0% . As highlighted in the figure, most of the solar collector yield is compensated by heat losses through the store and the piping. This situation can be nevertheless easily improved with modifications of the control.

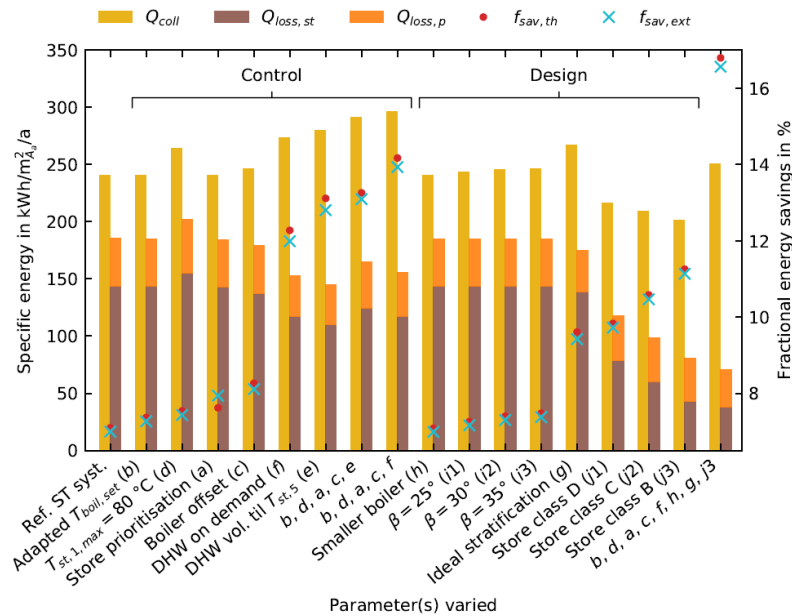


Fig. 6: Results of the TRNSYS simulations of the boathouse for several parameter variations and combinations.

The reduction of the boiler set-point (b) has a minor impact as it only slightly reduces the pipe losses in the SH loop. However an advantage that the simulation does not show is that in the real system this measure should avoid boiler overheating when the SH demand is very low, i.e. when the actually required SH inlet temperature is low (between 20 and $30 \text{ }^\circ\text{C}$), by preventing the boiler from starting up. The boiler entered several times in error mode during the winter 2017/2018 because of overheating as the SH demand was very low but the set-point temperature still had a value of $57.5 \text{ }^\circ\text{C}$. The increase of the maximum store bottom temperature $T_{st,5,max}$ (d) improves as expected the collector yield, but most of the gains occur outside of the heating season when the system enters daily in stagnation due to the low DHW demand. They are thus lost through higher store losses.

Giving priority to the store over the boiler (a) for SH also has a small impact. Indeed the store outlet to the space heating loop is located inside the DHW volume, which means that heat is delivered to the SH exclusively through the store. This contributes to reduce the running time of the boiler significantly as it does not continuously delivers to the space heating loop, but rather warms up the DHW volume when the minimal threshold is reached. This explains the improvement of $f_{sav,ext}$ seen in the figure. On the contrary, the short on/off boiler cycles might reduce its efficiency, which is however not assessed in the simulations. Taking into account the boiler offset (c) has a slightly higher impact on the performance thanks to the subsequent reduction of the DHW volume temperature which in turns reduces the yearly store losses.

The most impacting single measures are the ones reducing the size of the DHW volume (e and f) as they significantly reduce the store losses and leave more space for storing the heat from the solar collector loop. The worst $f_{sav,ext}$ in both cases is caused by a longer running time of the boiler, as it is the main direct supplier for the SH loop contrary to the previous cases when the supply is partly covered by the store (via the store outlet to the SH loop which was kept at a high temperature level as part of the DHW volume). As mentioned before however, the reduction of the number of boiler on/off cycles might improve the boiler efficiency but is not considered here. The DHW on demand only (f) performs worse than reducing the size of the DHW volume (e). It is the consequence of having the boiler offset not corrected in (f), which contribute to heating up a store volume at a higher temperature than simply keeping a smaller volume at the DHW set-point. The combination of e and f with the improvement of the control strategy shows on the contrary that DHW on demand is indeed the best solution compared to having a DHW volume, even a smaller one (110 litres).

All in all by simply modifying the control strategy, i.e. without any additional material cost, a doubling ($f_{\text{sav,ext}} = 13.9\%$) of the performance can be fulfilled.

The impact of the design of the system is also assessed. The reduction of the boiler size (*h*) does not bring any quantified improvement. Nevertheless, it contributes to lower the number of short boiler on/off cycles. Even though all fast oscillations of the outlet temperature are not completely avoided with a smaller boiler a significant reduction of their number and amplitude is noticeable. This should in the real system improve the boiler efficiency, but is not quantified in the present simulations. The tilt angle of the collector is also modified (*i*). However no real performance improvement is seen and this measure is hence not further considered as it would in the present case have led to additional costs for the mounting system without significant gains. The tiny improvement can be explained by the orientation of the boathouse (S53°W) which only leads to a 3.1 % increase of the total irradiation in the collector plane during the heating season (mid Sep. - mid May) when the tilt angle rises from 20° to 35°. With regards to system design, modifications of the store would bring the most significant improvements. A perfect stratification (*g*) plays an important role especially as in the boathouse case, the mixing occurs in the DHW volume (in its initial reference configuration of 370 l). Consequently the boiler needs to start-up in order to compensate for the cooling of the DHW volume. The heat content of the store increases therefore faster than without mixing, reducing the efficiency of the collectors (due to higher temperatures) but also decreasing the storage capacity available for the heat from the solar collector field. The reduction of the heat losses from the store is an additional way of increasing the fractional energy savings. This could be achieved through thicker insulation but also with reduction of the losses at the location of piping connections and temperature sensors. Finally combining the best assessed corrections of both control and design parameters would raise the extended fractional energy savings to 16.8 %. This is mainly achieved through a strong reduction of 74 % of the store losses and a minor 4 % increase of the solar collector gains compared to the reference solar thermal system.

4.2. Impact of the load profiles

As it was already mentioned in the previous sections, apart from the several issues detected during the monitoring phase, the major discrepancy between the actual system and the planned one is the incorrect assessment of the heat demand both for SH and DHW. In order to assess to which extent this affects the performance of the solar heating system, the profiles are varied. The resulting total yearly heat demands are detailed in Tab. 3.

Tab. 3: DHW and SH yearly energy needs for the different profiles simulated.

Profile name	DHW demand in MWh/a	SH demand in MWh/a
Ref. ST syst. Improved	0.58	19.68
DHW 80 l/d	1.16	19.68
DHW 120 l/d	1.76	19.68
DHW 160 l/d	2.33	19.68
DHW 200 l/d	2.93	19.68
0.75 SH	0.58	14.76
0.5 SH	0.58	9.84

All simulated variations bring the demands closer to the values foreseen during the planning phase compared to the actual ones. For DHW new profiles are randomly generated with DHWCalc with the indicated daily tapped volume at a temperature of 45 °C. The SH profiles are generated by multiplying the coefficient A from the measured sigmoid curves (eq. (1)) by the coefficient indicated in the profile name. Multiplying A by 0.5 for instance halves the total yearly heat demand when the other coefficients are kept constant. The calculation of the fractional energy savings also requires additional simulations of the reference conventional heating system with the varied load profiles. The results of the simulations are presented in Fig. 7. The solar heating system taken as reference on the left hand side of the figure corresponds to the system improved with modifications of the control strategy (variation “*b, d, a, c, f*” in Fig. 6), as these can be realistically implemented in the existing system contrary to the measures linked to the system design.

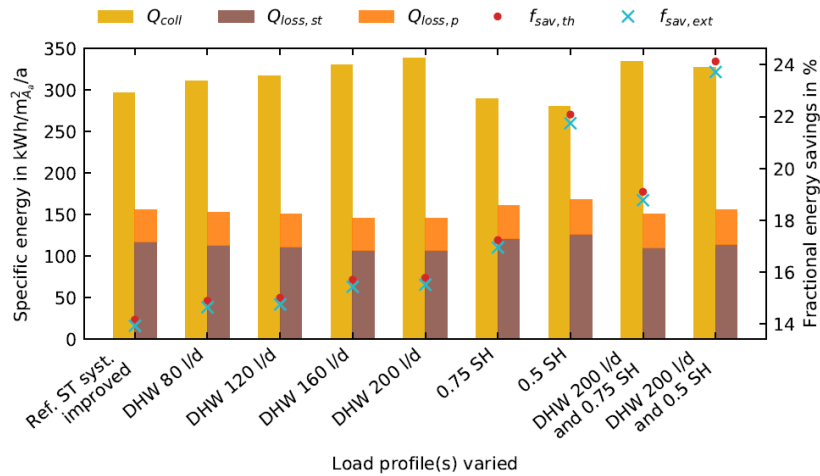


Fig. 7: Results of the TRNSYS simulations for the boathouse when varying the yearly DHW and SH demands.

It is first of all to notice that all simulated variations are increasing the savings. The rise of the DHW demand has the lowest impact but contributes to raise the contribution of the solar collector field, as it delivers more heat especially during summer time. A tapped volume of 200 l/d corresponds approx. to half of the foreseen yearly hot water needs. Further increase is not simulated as it does not seem very realistic that it will ever be reached given the current consumption level. Reducing the SH demand should be easier to fulfil with modifications of the control strategy of the AHU as highlighted before. Fig. 7 shows that it has the highest potential for increasing the fractional energy savings, even though the savings are lower in absolute values, which explains the lower solar thermal yield and slightly higher store losses compared to the reference. On top of increasing the fractional savings, the decrease of the SH demand obviously strongly reduces the needs for back-up energy and should be implemented in priority to lower the carbon footprint of the building. In the most favourable case simulated, with a halving of the SH needs and 5 times higher DHW demand, $f_{sav,ext}$ could reach 23.7 %, compared to 13.9 % with current consumption levels and at the same time the yearly energy delivered by the boiler would be reduced from 18.7 MWh/a to 10.9 MWh/a.

5. Costs analysis

The heat costs ($LCoH_{ov,fin}$) are also estimated. For this purpose, the methodology described in Louvet et al. (2018) is used. All prices mentioned here are net prices, without VAT. The period of analysis is 25 years and the real discount rate is taken equal to zero. No subsidy is considered. The investment (I_0) for the heating system is based on actual prices including both material and installation. The material prices for the boiler (3000 €), collectors (200 €/m^2_{AG}), collector connections (20 €/piece) and collector mounting system (40 €/m^2_{AG}) were unknown from the project and the value given in parenthesis are estimated from average component prices found on the internet. With the same method a price of 250 € is taken for the buffer store of the reference conventional heating system with additional installation costs of 500 €. Under these assumptions, the total investment for the solar part of solar assisted heating system amounts to 15 131 € (including the credit of 750 € from the store of the reference conventional system) and 13 485 € for the conventional part. The breakdown of the costs is shown in Fig. 8. The maintenance costs are calculated at the component level, with the values given in VDI (2012). The yearly maintenance cost for each component is the sum of the yearly effort for maintenance, servicing and inspection indicated in the reference. The replacement costs are also added for each component depending on their given depreciation period (VDI, 2012) and equally spread over the period of analysis. The rest value is deduced from the replacement costs if the component (or replaced component) depreciation period exceeds the period of analysis. As additional assumption, the total yearly maintenance effort for the PP storage were reduced from 2 % to 1 % of the investment as less maintenance is required than for conventional metallic buffer stores. Under these assumptions, the total maintenance costs for the solar part of the solar assisted heating system amount to 253 € (1.7 % of I_0) and 295 € for the conventional part (2.2 % of I_0).

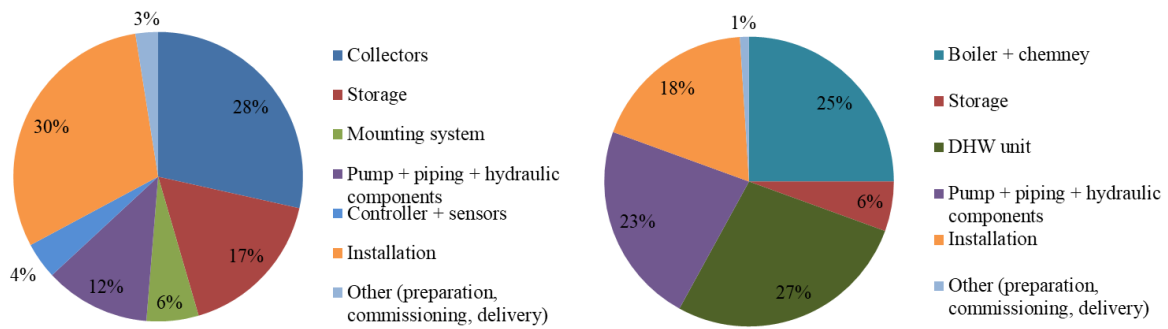


Fig. 8: Breakdown of the investment costs for the solar part (left) and conventional part (right) of the solar assisted heating system installed at the boathouse.

The calculated heat costs are presented in Fig. 9 and one can notice that they are in all cases higher for the solar assisted heating system compared to the reference conventional system. Without any improvement, the heating system with solar assistance has a $LCoH_{ov,fin}$ 30 % higher than the reference conventional system, which drops to 26 % with the improvement of the control and decreases further to 24.5 % with additional design improvements (Fig. 9, left). This example also highlights that despite a more than doubling of the saved final energy between the worst (Ref. ST syst.) and the best (b, d, a, c, f, h, g, j₃) cases investigated, the $LCoH_{ov,fin}$ faces a slight reduction of only 4.5 %. This is a consequence of the small share of the total energy supply which is covered by the solar heating system.

The load profiles have as expected an important impact on the heat costs. For both systems (solar and reference), the rise of the heat consumption decreases the heat costs and vice-versa. In the former case indeed, the weight of the investment costs per unit of energy is reduced which explains the lower heat costs. Moreover, while the increase of the DHW consumption has a positive impact in bringing closer the $LCoH_{ov,fin}$ of both systems, the reduction of the SH load has the opposite effect.

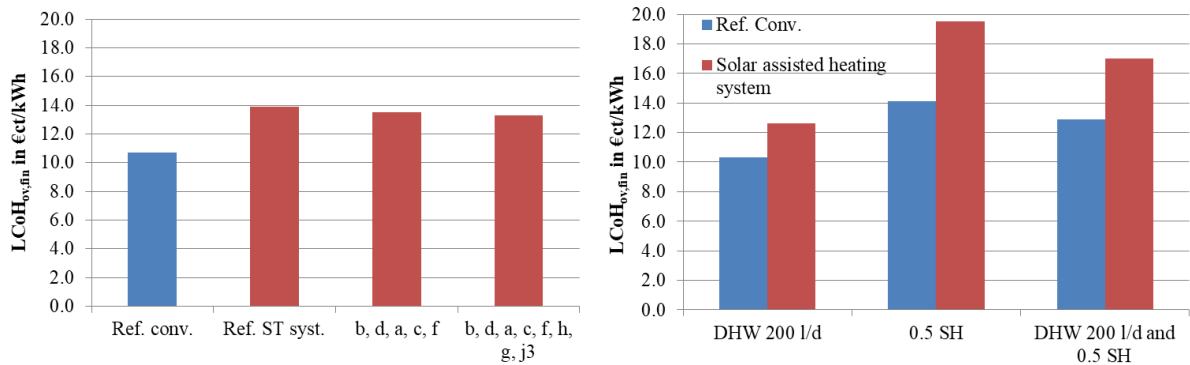


Fig. 9: $LCoH_{ov,fin}$ for different parameter configuration of the solar assisted heating system compared to one of the reference conventional system (left) and comparison of the $LCoH_{ov,fin}$ of solar assisted heating system (with improvements b, d, a, c, f) and the reference conventional system for varying load profiles.

6. Discussion and conclusion

The analysis revealed a poor performance of the system after commissioning but showed that most of the issues identified could be solved through an adapted control strategy, already significantly raising the performance. The unusual usage of the building contributes to the specificity of the most energy efficient control strategy determined with the simulations. Indeed no DHW volume should be kept in the store and DHW only prepared on-demand. This would however require that the building users adapt to this uncommon situation and this solution was not adopted for this reason. In addition to the control strategy, additional care in the system design, notably regarding store stratification and heat losses could further improve the system performance. A smaller boiler would also be more adapted and avoid overheating and short on/off cycles.

The measurements have shown that the solar thermal system with current DHW consumption level is over-dimensioned which also partly explains the low specific collector yields. Beyond this fact the drainback design

appears as an appropriate technical solution for such a building with very low consumption during summer time causing collector stagnation almost every day. A conventional pressurized system would result in a much higher stress on the components of the solar collector loop due to high temperatures and pressures and lead to a fast degradation of the HTF. This would in turn lead to higher maintenance efforts especially as antifreeze mixtures might account for most of the required maintenance (Schiebler, 2018).

On top of preventing damaging stagnation cycling, the chosen drainback design is perfectly suited for heating systems as the one installed at the boathouse. Indeed, as it is notably highlighted in R. Botpaev et al. (2016) and Ruslan Botpaev (2017), DBS require additional care by planning and installation in order to ensure proper filling, operation and draining. At the boathouse, the heat storage, which is also the drainback tank, is located directly under the roof in the attic. The collector loop can thus be filled without the need to over-dimension the pump. Moreover a reduction of the water boiling point due to underpressure is also avoided. The risk associated with an incorrect installation of outside piping nevertheless remains. The boathouse highlights the necessity to avoid using flexible pipes with drainback systems in (almost) horizontal sections. Rigid piping should be installed instead.

Despite the apparent simplicity of such system, due to fewer components thanks to the drainback design in the solar collector loop and the reduction of the number of heat exchangers, the costs analysis showed that with the current consumption level the heat costs are between 24.5 and 30 % higher with the solar assistance than without, depending on the control and design improvements considered. This can be partly explained by the very low DHW-consumption which limits the solar yield outside of the heating period. A better estimation of the needs is therefore a key to reduce the heat costs. It nevertheless also appears that further reductions of the investment costs are required to increase the competitiveness of combi-systems.

7. References

- BDEW, 2015. BDEW/VKU/GEODE Leitfaden - Abwicklung von Standardlastprofilen Gas. BDEW, VKU, GEODE, Berlin.
- Botpaev, R., Louvet, Y., Perers, B., Furbo, S., Vajen, K., 2016. Drainback solar thermal systems: A review. *Sol. Energy, Special issue: Progress in Solar Energy* 128, 41–60. <https://doi.org/10.1016/j.solener.2015.10.050>
- CEN, 2012. EN 12977-2:2012 Thermal solar systems and components – Custom built systems – Part 2: Test methods for solar water heaters and combisystems. European Committee for Standardization (CEN), Brussels, Belgium.
- Deutscher Bundestag, 2016. Sachstand - Primärenergiefaktoren (No. WD 5-3000-103/16). Wissenschaftliche Dienste - Deutscher Bundestag.
- DIN, 2016. DIN EN 12897 - Wasserversorgung – Bestimmung für mittelbar beheizte, unbelüftete (geschlossene) Speicher-Wassererwärmer. Deutsches Institut für Normung, Berlin.
- European Commission, 2013. Commission delegated regulation (EU) No 812/2013 of 18 February 2013 supplementing Directive 2010/30/EU of the European Parliament and of the Council with regard to the energy labelling of water heaters, hot water storage tanks and packages of water heater and solar device. Brussels, Belgium.
- Hellwig, M., 2003. Entwicklung und Anwendung parametrisierter Standard-Lastprofile (PhD Thesis). TU München, Munich.
- IWU, 2018. IWU-Tools / Werkzeuge - Gradtagszahlen in Deutschland [WWW Document]. URL <http://www.iwu.de/downloads/tools/> (accessed 14.02.2018).
- Jordan, U., Vajen, K., 2005. DHWcalc: Program to generate domestic hot water profiles with statistical means for user defined conditions, in: *Proceedings of the 2005 Solar World Congress Bringing Water to the World*. Orlando, Florida, USA.
- Klein, S.A., Beckman, W.A., Mitchell, J.W., 2006. TRNSYS 16 a TRaNsient SYstem Simulation program.
- Louvet, Y., Fischer, S., Furbo, S., Giovannetti, F., Köhl, M., Mauthner, F., Mugnier, D., Philippen, D., Veynandt, F., 2018. LCOH for Solar Thermal Applications (No. Info Sheet A01). IEA SHC - Task 54 Price Reduction of Solar Thermal Systems. URL <http://task54.iea-shc.org/info-sheets> (accessed 15.11.2018).
- Schiebler, B., 2018. Cost reduction by temperature limitation. SHC Solar Academy Webinar. URL <https://www.youtube.com/watch?v=5aNeDR6bfHY> (accessed 15.11.2018).
- VDI, 2012. VDI 2067, Blatt 1 - Wirtschaftlichkeit gebäudetechnischer Anlagen Grundlagen und Kostenberechnung. Verein Deutscher Ingenieure (VDI), Düsseldorf, Germany.